ID: 2910

The effect of gas puffing at the LH grill on the efficiency of the central dense plasma ion heating at the FT-2 tokamak

D.V. KOUPRIENKO, A.B. ALTUKHOV, D.YU. BATYREV, M.V. DERYABINA, V.V. DYACHENKO, L.A. ESIPOV, A.D. GURCHENKO, E.Z. GUSAKOV, M.A. IRZAK, M.YU. KANTOR, E.O. KISELEV, A.N. KONOVALOV, S.I. LASHKUL, A.YU. POPOV, S.V. SHATALIN

Ioffe Istitute

denis.kouprienko@mail.ioffe.ru

MOTIVATION

The gas puffing, commonly employed to achieve effective coupling between the grill antenna and the plasma, is expected to provide:

- a stabilizing effect that suppresses Parametric Decay Instabilities (PDI) by increasing the collision frequency;
- formation of the slow-wave spectrum (refractive index N_z) generated by the antenna's retarding system;
- increase of the efficiency of Lower Hybrid Current Drive (LHCD) and Lower Hybrid Heating (LHH) by creating a more favorable slow-wave spectrum (N_z).

Presented work: variation of the gas puffing valves versus LH grill position.

High efficiency of central ion heating is observed, which depends significantly on gas puffing scenario.

The formation of a strongly non-monotonic density profile is observed during LH pulse. Two mechanisms are discussed as potential causes of this effect: the influence of ponderomotive forces and ITB formation

Experimental/modeling approach

FT-2 tokamak: a = 0.08 m, R = 0.55m, I_{pl} ~ 30-35 kA, B_T ~ 2.2 T, q_{95} ~ 3-3.5

- Lower hybrid heating (LHH): P_{LH} = 100 kW, f_{LH} = 920 MHz
- ASTRA code transport modeling based on the experimental data

Basic diagnostics:

T_e, n_e – thomson scattering, full profile;

T_i – charge exchange; n_e – interferometer, full profile;

Langmuir, electrostatic and magnetic probes.

PDI (parametric decay instabilities)

In high density regimes the first satellite amplitude depends on the position of the gas puffing relative to the grill position

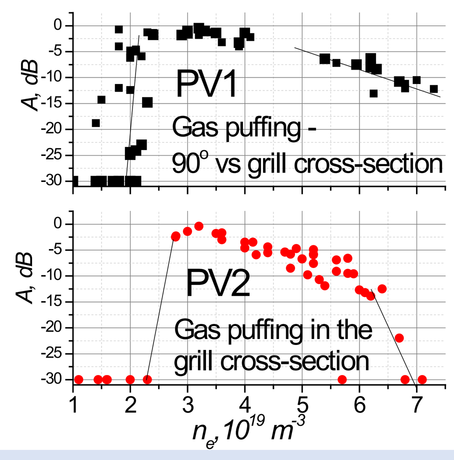

LHH scenario. Reconstruction of magnetic configuration of non-monotonic density profiles

High density plasma scenario

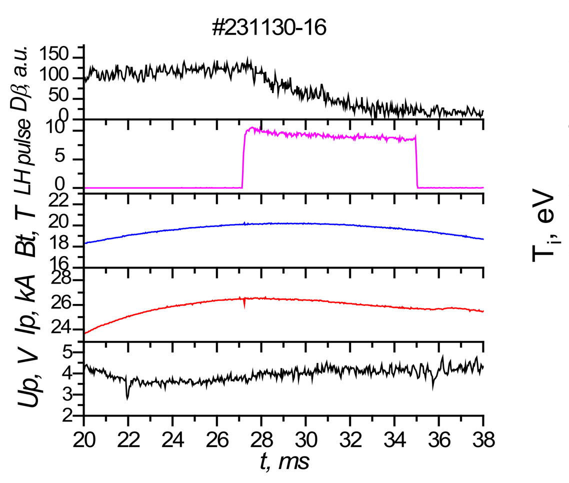

LHH discharge scenario. Loop voltage Up, plasma current Ip, toroidal field Bt, LH pulse and D_α line emission

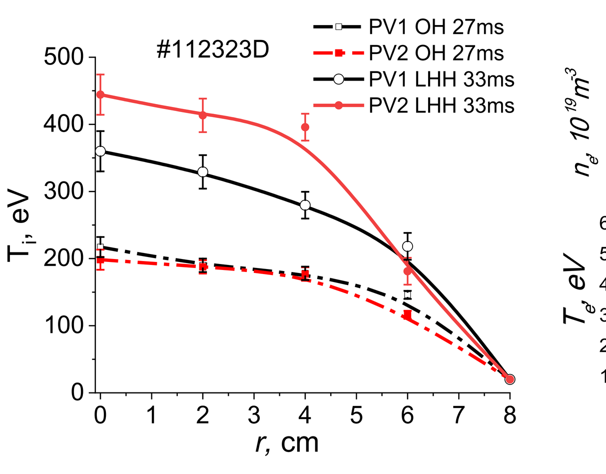

Ion temperature: comparison of ion heating at pulsed gas puffing via valves PV1 and PV2

Strongly non-monotonic density profiles, induced by LHH

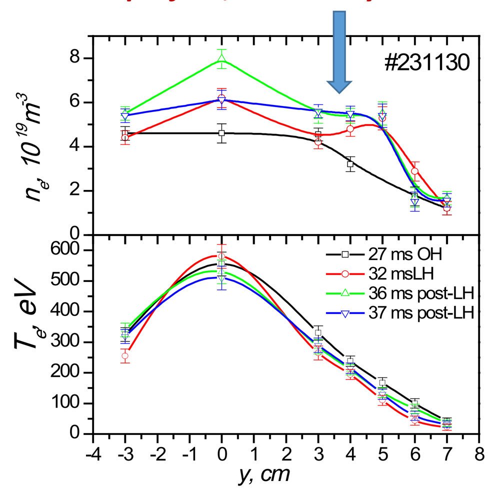

PV2 case. $T_e(r)$ and $n_e(r)$ profiles during LHH: ohmic, LH and post-LH stages

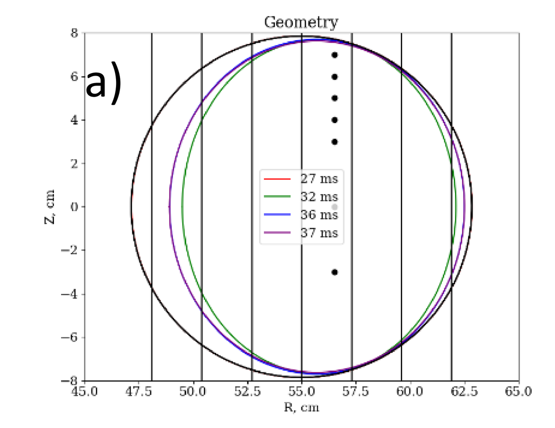

the plasma boundary for each case OH, LH and post-LH

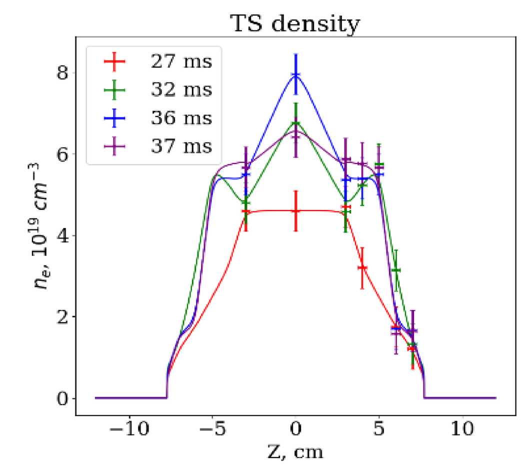

the electron density along with TS experimental data points

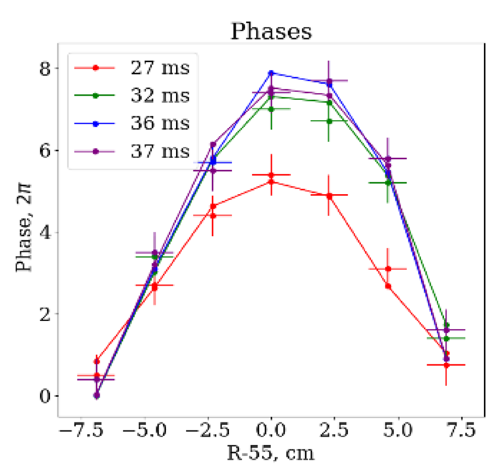

the interferometer phases

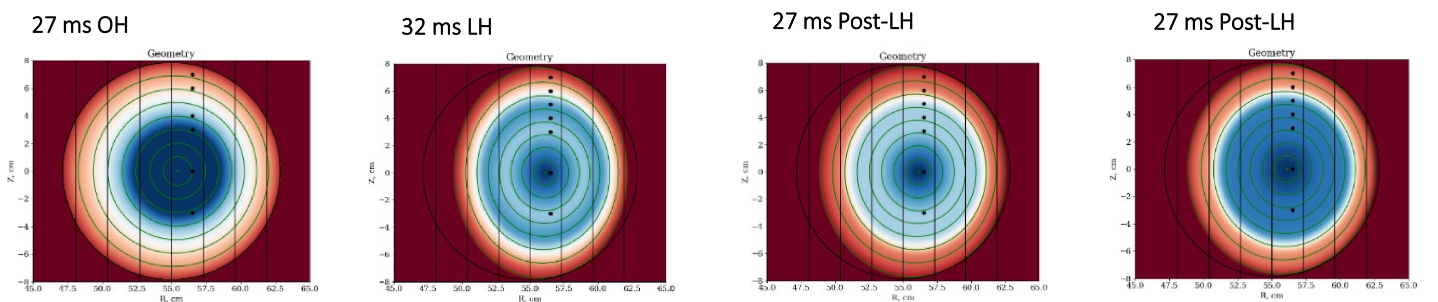

Density distribution throughout the entire plasma volume

Possible role of magnetic islands

MHD signal drop after switching off LH pulse

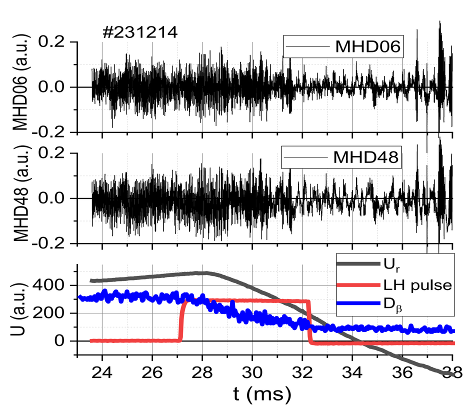

The signals from MHD probes 06 and 48 during LHH

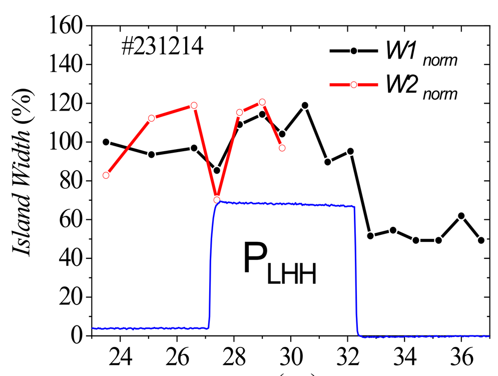

Dynamics of normalized island widths *W1* and *W2* (black and red) during LH pulse (blue) over time

MHD is Not a reason of measured non-monotonic density profiles

REFERENCES

1. V.E. Golant, V.I. Fedorov. High-frequency methods of plasma heating in toroidal fusion devices (in Russian), (Energoatomizdat, M., 1986), pp. 69–96, 116–141
2. S.I. Lashkul, A.B. Altukhov, A.D. Gurchenko, et al., Technical Physics Letters, (2024), Vol. 50, No.3. pp. 73-76
3. S.I. Lashkul, A. B. Altukhov, A. D. Gurchenko et al., Plasma Physics Reports, (2020), Vol. 46, No. 9, pp. 863–873
4. C. Castaldo, A. Di Siena, R. Fedele et all. Nuclear Fusion 56 (2016) 016003
5. A.V. Sidorov et al., Technical Physics, 2022, Vol. 92, No. 4
6. G. Pereverzev and P. Yushmanov, Report No. 5/98. (Max-Planck-Institut für Plasmaphysik, Garching, 1998)
7. H. R. Wilson (2006) Neoclassical Tearing Modes, Fusion Science and Technology, 49:2T, 155-163. https://doi.org/10.13182/FST06-A1115
8. S.V. Shatalin, E.O. Vekshina, P.R. Goncharov, et al., Plasma Physics Reports, 2004. Vol. 30, No. 5, pp. 363–369.
9. A. Zabolotsky, H. Weisen and TCV Team. Plasma Phys. Control. Fusion 48 (2006) 369–383 doi:10.1088/0741-3335/48/3/003
10. V.A. Petrzilka, F. Leuterer, F.-X. Soldner et al., Nucl. Fusion, 1991, Vol. 31, p. 1758. doi: 10.1088/0029-5515/31/9/014.
11. V.I. Karpman, A.G. Shagalov J. Plasma Physics. 1982. V.27. P. 215. doi: https://doi.org/10.1017/S0022377800026544.
12. M.A. Irzak, O.N. Shcherbinin Nucl. Fusion. 1995 V. 35 P. 1341. doi: 10.1088/0029-5515/35/11/I02.
13. A.G. Litvak, in Reviews of Plasma Physics, edited by M. A. Leontovich (Consultants Bureau, New York) (1986), vol. 10, p. 293.

CONCLUSIONS

Increase in the efficiency of ion heating was observed when the working gas was injected through the grill port, leading to stabilization of the parametric decay instability of the LH wave [3, 4].

The formation of a non-monotonic density profile during LHH was detected.

Two possible factors causing this effect are considered: ITB formation and ponderomotive forces. A more probable explanation is that the ponderomotive effect could be a trigger for the plasma density profile transformation, but the ITB formation during LHH is more likely to explain the observed effects.

The modification of edge plasma parameters due to the ponderomotive force is expected to play a significant role in future large-scale facilities at high power levels, impacting the antenna-plasma coupling efficiency.

Ponderomotive effects at the LH heating

Plasma core: modelling

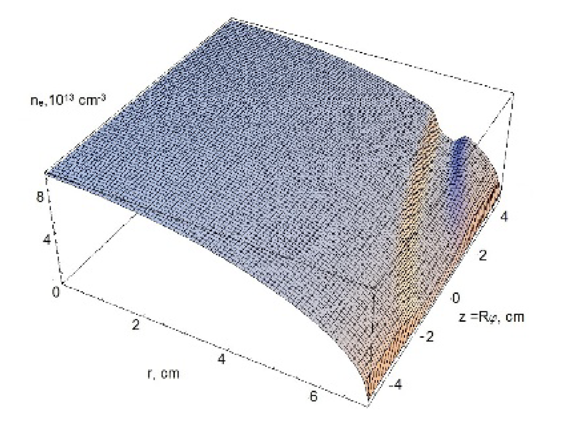

Oblique propagation of the microwave beam from the point of pump wave injection

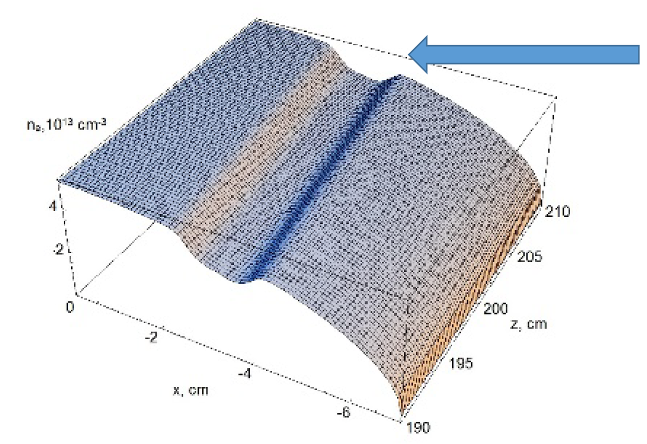

The same as left, but displaced by 180° along the major circumference from the point of microwave beam injection

LH waves form a structure of the resonant cone type

Plasma SOL: Langmuir probe measurements

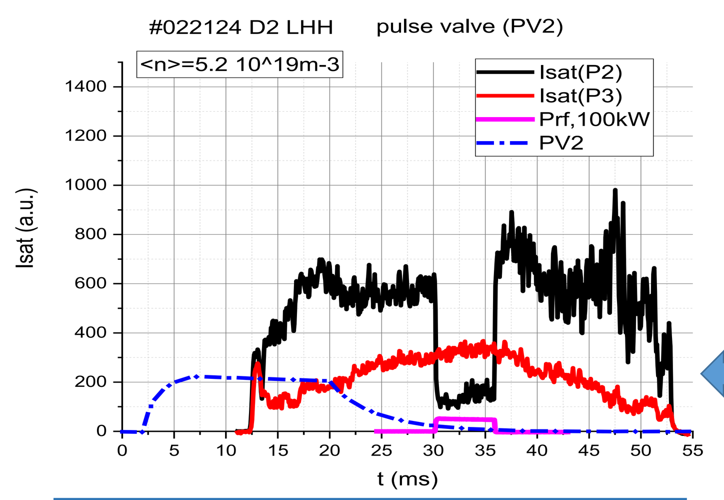

Comparison of I_{sat} collected by the RF probe (P2) and the toroidally displaced movable probe (P3). The dash-dotted line indicates the timing of the triggering pulse for the gas injection valve PV2.

plasma density drop in the SOL during LH pulse

Ponderomotive force:

$$f_M = -\nabla\Phi$$

$$n\Phi = \frac{\omega_{pe}^2}{\omega^2}\frac{E_\parallel^2}{8\pi} + \frac{\omega_{pe}^2}{\omega^2-\omega_{ce}^2}\frac{E_\perp^2}{8\pi}$$

The electron density in the region opposite the LH grill:

$$n \approx n_e\left(1-\int_{-v_m}^{v_m}\exp\left(-\frac{v^2}{v_{T_e}^2}\right)\frac{dv}{\sqrt{\pi}v_{T_e}}\right) = n_e\left(1-\frac{\delta n}{n_e}\right) = n_e\left(1-\mathrm{erf}\left(\sqrt{\frac{2\Phi_{max}}{m_e v_{T_e}^2}}\right)\right)$$

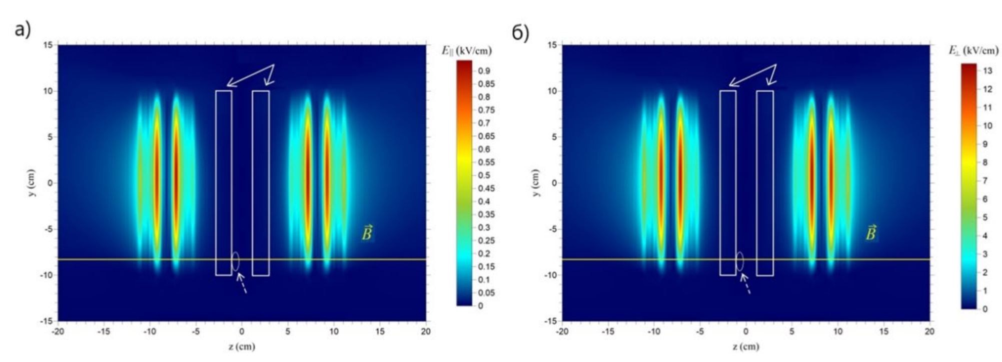

The distributions of (a) the parallel and (b) the perpendicular components of the electric field in the plane where the probe is located. The yellow straight line is a magnetic field line with the magnetic induction vector B. The arrows indicate the grill waveguides. The small ellipse marks the position of the RF probe.

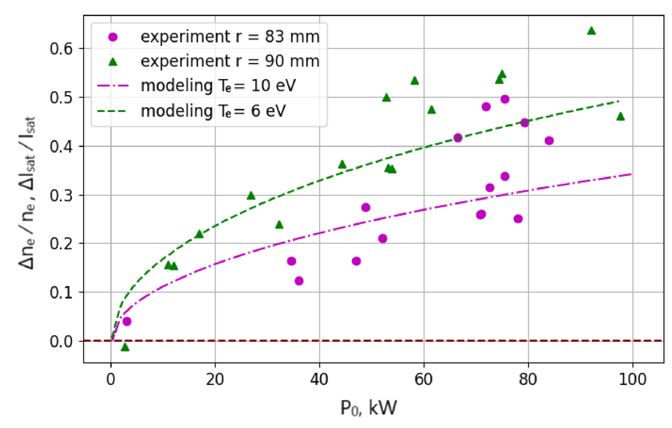

Dependence of the experimental values of $\Delta I_{sat}/I_{sat}$ and the calculated results for $\Delta n/n$ on the LH power.

ITB modelling

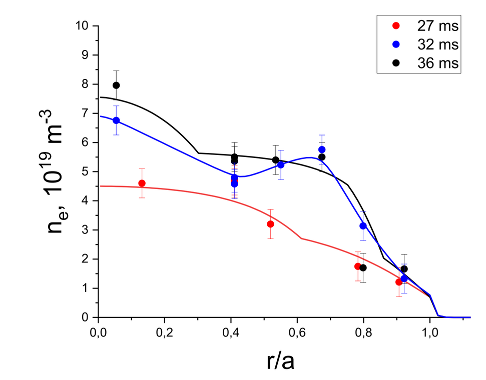

$$\frac{1}{V'}\left(\frac{\partial}{\partial t}-\frac{\dot{B}_0}{2B_0}\frac{\partial}{\partial\rho}\rho\right)(V'n_e)+\frac{1}{V'}\frac{\partial}{\partial\rho}\Gamma_e = S_e,$$

$$\begin{pmatrix}\frac{\Gamma_e}{n_e}\\ \frac{q_e}{n_eT_e}\\ \frac{q_i}{n_iT_i}\\ V'G_1\frac{\mu_0 j_{BS}}{B_p}\end{pmatrix} = -V'G_1\begin{pmatrix}D_n & D_e & D_i & D_E\\ \chi_n^e & \chi_e & \chi_i^e & \chi_E^e\\ \chi_n^i & \chi_e^i & \chi_i & \chi_E^i\\ C_n & C_e & C_i & 0\end{pmatrix}\cdot\begin{pmatrix}\frac{1}{n_e}\frac{\partial n_e}{\partial\rho}\\ \frac{1}{T_e}\frac{\partial T_e}{\partial\rho}\\ \frac{1}{T_i}\frac{\partial T_i}{\partial\rho}\\ \frac{E_\parallel}{B_p}\end{pmatrix}$$

$$S_e = s_{ion}^{(e)}Nn_e + s_{ion}^{(i)}Nn_i - s_{rec}n_in_e$$

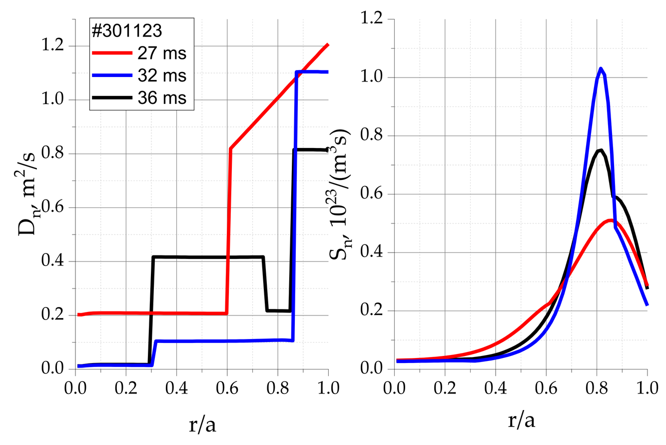

diffusion coefficients D, m²/s, and particle source intensity S, m³/s

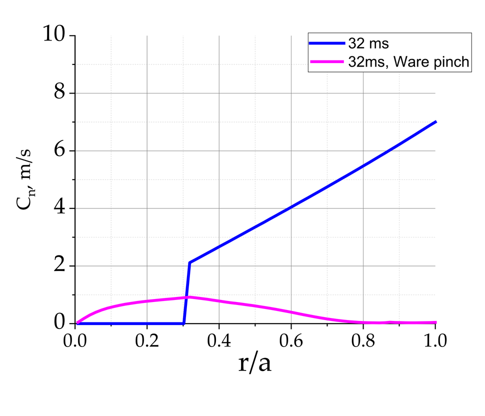

pinch particle velocity C_n, m/s, for 32m

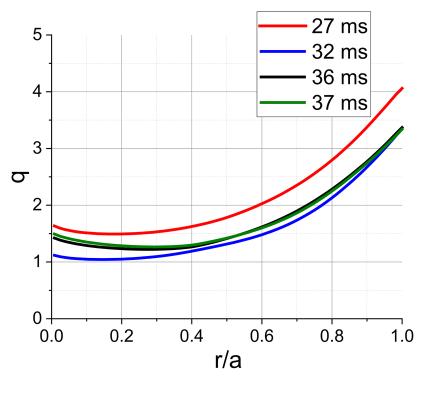

safety factor (q) profile

ACKNOWLEDGEMENTS

The financial support of the Ioffe Institute state contracts № FFUG- 2021-0001 and № FFUG- 2024-0028 is acknowledged